Biomaterials 30 (2009) 5622–5630

Contents lists available at ScienceDirect

Biomaterials

journal homepage: www.elsevier.com/locate/biomaterials

Optical and biological sensing capabilities of Au_2S/AuAgS coated gold nanorods

Haowen Huang [a,c,*], Xuanyong Liu [b,c], Yunlong Zeng [a], Xianyong Yu [a], Bo Liao [a], Pinggui Yi [a], Paul K. Chu [c,**]

[a] School of Chemistry and Chemical Engineering, Hunan University of Science and Technology, Xiangtan 411201, China
[b] Shanghai Institute of Ceramics, Chinese Academy of Science, Shanghai 200050, China
[c] Department of Physics & Materials Science, City University of Hong Kong, Tat Chee Avenue, Kowloon, Hong Kong

ARTICLE INFO

Article history:
Received 23 April 2009
Accepted 26 June 2009
Available online 21 July 2009

Keywords:
Biological sensing
Nanorods
Functionalization
Au_2S/AuAgS coated gold nanorods
Core–shell nanostructure
Optical properties

ABSTRACT

Gold nanorods coated with a multiplex component, namely Au_2S/AuAgS coated gold nanorods, are produced without precipitation and aggregation among the nanorods. Both the thickness of the shell and size of the core can be readily controlled by this technique allowing one to tune the plasmon resonance of the nanocomposites over a range of several hundred nanometers. These Au_2S/AuAgS coated gold nanorods exhibit interesting optical properties and are suitable for many biological sensing applications. Functionalization of the Au_2S/AuAgS coated gold nanorods is achieved by manipulating the affinity between the Au_2S/AuAgS and thiol compounds. Biomolecules can be covalently attached via the NH_2 bond of the antibodies to the NHS-terminated nanorods. The longitudinal peaks of the Au_2S/AuAgS coated gold nanorods are extremely sensitive to the refractive index changes induced by target binding, suggesting that they are excellent sensors for target-specific binding events and have the potential to achieve single-molecule sensitivity in microspectroscopy.

1. Introduction

In recent years, there has been significant interest in nanocomposite materials consisting of assembled molecules or nanosized inorganic objects in biomaterials research [1–3]. In particular, hybrid structures based on inorganic nanocrystals are becoming increasingly attractive due to the strong dependence of their optoelectronic, magnetic, catalytic, and sensing properties on the size, shape, and composition. Recent advances in colloidal syntheses have revealed the possibility of producing gram-scale amounts of nanoparticles with elaborate shapes to serve as the building blocks of future materials and nanodevices [4–6]. Incorporation of different functional units into the same nanoparticle structure is expected to result in novel or amplified physical–chemical properties paving the way for the development of nanosized entities that are able to perform multiple technological tasks such as those required by biomedical engineering, diagnostics, pharmaceutics, and biosensing [7–11].

Gold nanorods (GNRs) are elongated nanoparticles with distinctive optical properties that depend on their shape. Owing to the structural geometry, these structures are useful in biological sensing, imaging, and therapy. However, the use of GNRs as biosensors for analytes has not yet been widely pursued. This is because the cetyltrimethylammonium bromide (CTAB) layer on the GNR surface cannot be easily displaced by the biomolecules of interest [12,13]. It is thus necessary to develop new surface chemistry that will render them amenable to surface functionalization, bioconjugation, and assembly. There are currently two different heterostructure design methodologies. One strategy involves careful selection of the molecules that can provide the suitable functional groups to preferentially or selectively bind to the desired nanoparticle type, which leads to the spontaneous formation of assemblies with varying degrees of spatial order [14–16]. The second approach relies on epitaxial growth of different materials by delicate control of parameters such as surface reactivity, interfacial energy, and crystal solubility on the nanoscale [17–20]. However, regardless of the technique, synthesis of core–shell structures by conventional physical blending or chemical precipitation followed by surface adsorption usually produces insoluble materials. Hence, precise control of the size, morphology, and dispersion of the metal component are inherently difficult. Furthermore, conventional protocols usually involve many elaborate steps thereby making accurate control even more arduous. Consequently, reduced conversion yields and/or loss of colloidal stability ensue and preparation of metal heterostructures in a controllable fashion are quite challenging. In this paper, we report a novel concept to fabricate core–shell structures consisting of gold nanorods coated

* Corresponding author. School of Chemistry and Chemical Engineering, Hunan University of Science and Technology, Xiangtan 411201, China.
** Corresponding author.
E-mail addresses: hhwn@iccas.ac.cn (H. Huang), paul.chu@cityu.edu.hk (P.K. Chu).

0142-9612/$ – see front matter © 2009 Elsevier Ltd. All rights reserved.
doi:10.1016/j.biomaterials.2009.06.060

with multiplex components, namely Au_2S/AuAgS coated gold nanorods and discuss possible biological sensing applications.

2. Materials and methods

2.1. Materials

Hydrogen tetrachloroaurate ($HAuCl_4 \cdot 3H_2O$, ≥99.99%), $AgNO_3$, $NaBH_4$, $Na_2S_2O_3$, cetyltrimethylammonium bromide (CTAB), and ascorbic acid were purchased from Sinopharm Chemical Reagent Co., Ltd (Shanghai, China). Other reagents included *N*-hydroxysuccinimide (NHS) from ACROS (New Jersey, USA), *N*-ethyl-*N*-[(dimethylamino) propyl]carbodiimide (EDC) from Avocado Research Chemicals Ltd (Lancashire, UK), mercaptoundecanoic acid (MUA) from Aldrich (Milwaukee, USA). The bovine serum albumin, goat IgG, and rabbit anti-goat IgG were obtained form Biodee Biotechnology Co., Ltd (Beijing, China). Doubly distilled water was used in all the experiments.

2.2. Synthesis of gold nanorods

The gold nanorod seed solution was prepared according to previous methods with slight modification [21,22]. The CTAB solution (1.5 mL, 0.1 M) was mixed with 100 μL of 0.02 M $HAuCl_4$ and 100 μL of ice-cold 0.01 M $NaBH_4$ was added while being stirred resulting in the formation of a brownish yellow solution. Rigorous stirring of the seed solution continued for 2 min. The seed solution was kept at room temperature (25 °C) and used at least 2 h after its preparation.

To grow the gold nanorods, 1.5 mL of 0.02 M $HAuCl_4$ and 0.8 mL of 0.01 M $AgNO_3$ were added into 30 mL of 0.1 M CTAB, followed by the addition of 0.8 mL 0.08 M ascorbic acid (slightly in excess). Ascorbic acid worked as a mild reducing agent and changed the growth solution from dark yellow to colorless. Finally, 70 μL of the seed solution was added to the solution. The color of the solution gradually changed within 15 min.

2.3. Fabrication of Au_2S/AuAgS coated gold nanorods

The gold nanorods were synthesized by the seeding growth method in an aqueous CTAB solution. 50 μL of a 1 M Na_2S solution was added into 3 mL of the as-synthesized gold nanorods at room temperature, heated, and kept at 50 °C. Absorption spectroscopy was conducted on the resulting nanorods on the Lambda 35 (Perkin Elmer). Because the longitudinal plasmon wavelength (LPW) of the resulting nanorods red shifted with increasing reaction time, various Au_2S/AuAgS coated gold nanorods were acquired at different reaction time intervals during which the mixture of gold nanorods and Na_2S solution was taken out, cooled to room temperature rapidly in ice water, centrifuged, and re-dispersed in an aqueous solution.

2.4. Functionalization of Au_2S/AuAgS coated gold nanorods and immunochemistry

The MUA monolayers were formed on the Au_2S/AuAgS coated gold nanorods in a 5 mM ethanol solution for at least 18 h, followed by thorough rinsing with ethanol and water. The modified nanorods were bonded to NHS by immersing in an aqueous solution of 75 mM EDC and 15 mM NHS for 30 min. In order to attach biological macromolecules on the surface, the NHS-terminated nanorods were incubated in a goat IgG solution (0.01 g/L) and BSA solution (0.01 g/L). After reacting for about 30 min, the nanorods were rinsed with PBS and then blocked by 1 M ethanolamine (pH = 8.5) for 10 min.

2.5. Electron microscopy

Transmission electron microscopy (TEM) was carried out on a JEM-2010 transmission electron microscope at 80 kV. X-ray photoelectron spectroscopy (XPS) was conducted using the ESCALab201i-XL spectrometer (VG Scientific Ltd., East Grinstead, Sussex, UK). The base pressure during acquisition was about 3×10^{-7} Pa and the C1s line (284.6 eV) was used for energy calibration. The X-ray diffraction (XRD) data were obtained on a Siemens D5000 diffractometer equipped with the Cu $K_{\alpha 1}$ ($\lambda = 1.54056$ Å) X-ray source and analyzed using Traces Software. Energy-dispersive X-ray spectroscopy was carried out at 25 kV using a JEOL JSM-6380LV field-emission scanning electron microscope (FEI Co.). The extinction spectra were obtained using the Lambda 35 (Perkin Elmer) and the resonance light scattering spectra were acquired on the F-4500 fluorescence spectrometer (Hitachi, Japan).

3. Results and discussion

3.1. Fabrication and characterization of Au_2S/AuAgS coated gold nanorods

Several parameters such as the amount of seed can be altered in this method to adjust the geometry of the particles and consequently the optical response. In order to fabricate the formation of the core–shell nanocomposite, an excess of 1 M freshly prepared Na_2S aqueous solution was mixed with the GNRs. The mixture was stirred in a vessel exposed to air towards the end of the reaction and the color of the solution changed gradually from wine red to pale green. Fig. 1 shows the temporal evolution of the GNRs reacting with Na_2S at a constant temperature of 60 °C. The GNRs initially exhibit one band around 520 nm attributable to the transverse plamson wavelength (TPW) and another band at a longer wavelength corresponding to the longitudinal plasmon wavelength (LPW). A chalcogenide layer is probably formed on the GNR surface in the reaction. The resulting nanoparticles are characterized by transmission electron microscopy (TEM). Fig. 2 shows the micrographs of the as-synthesized GNRs and resulting nanocomposites. The two different phases can be ascribed to the chalcogenide layer covering the GNR and reduced GNR core. The metal chalcogenide layer is a narrow band gap semiconductor with a large refractive index at typical optical frequencies. The LPW should produce red shifts if the larger refractive index chalcogenide layer covers the GNRs. As expected, a continuous red shift in the LPW accompanied by reduced intensity is observed with longer reaction time as shown in Fig. 1. The final LPW of the nanorods depends on the reactant concentration, temperature, and reaction time.

This protocol can be readily scaled up to prepare gram-scale chalcogenide coated gold nanorods. In order to confirm the components and structure of the nanocomposite, X-ray photoelectron spectroscopy (XPS) is performed and the results are shown in Fig. 3. In addition to Au and S, elemental Ag is found in the nanorods. The small quantity of Ag arises from the addition of $AgNO_3$ which allows better control of the shape of the synthesized GNRs, as shown in Fig. 4. Fig. 5 compares the XRD spectra obtained from the as-synthesized GNRs, and nanocomposite. The Au_2S and AuAgS can be identified according to previous reports [23–28]. The unlabeled peaks may originate from the CTAB remaining on the nanocomposite, and the shell enshrouding the GNR consists of multiplex components including Au_2S and AuAgS. According to our experimental data, the shell appears to consist of primarily Au_2S together with a small fraction of AuAgS. Here, this nanocomposite structure is referred to as Au_2S/AuAgS coated gold nanorods. Formation of this core–shell structure is a result of the as-synthesized GNRs being corroded gradually by Na_2S from the outside. This is different from the conventional formation mechanism of a core–shell structure by gradually coating the shell onto the unaltered starting nanorods. These GNRs are capsulated by CTAB micelles and

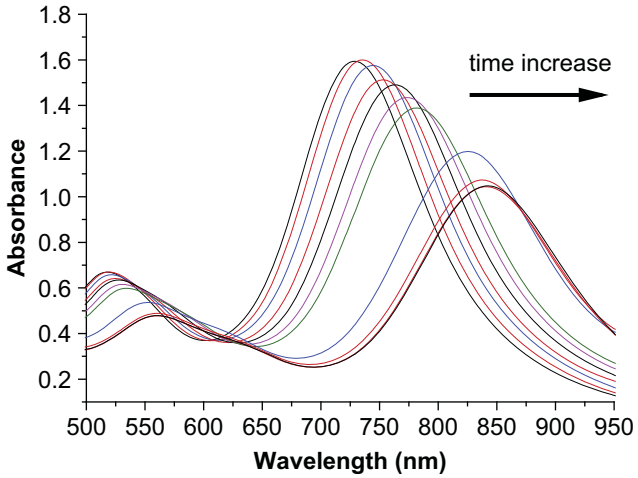

Fig. 1. Extinction spectra acquired from the as-synthesized gold nanorods reacting with Na_2S for different time durations.

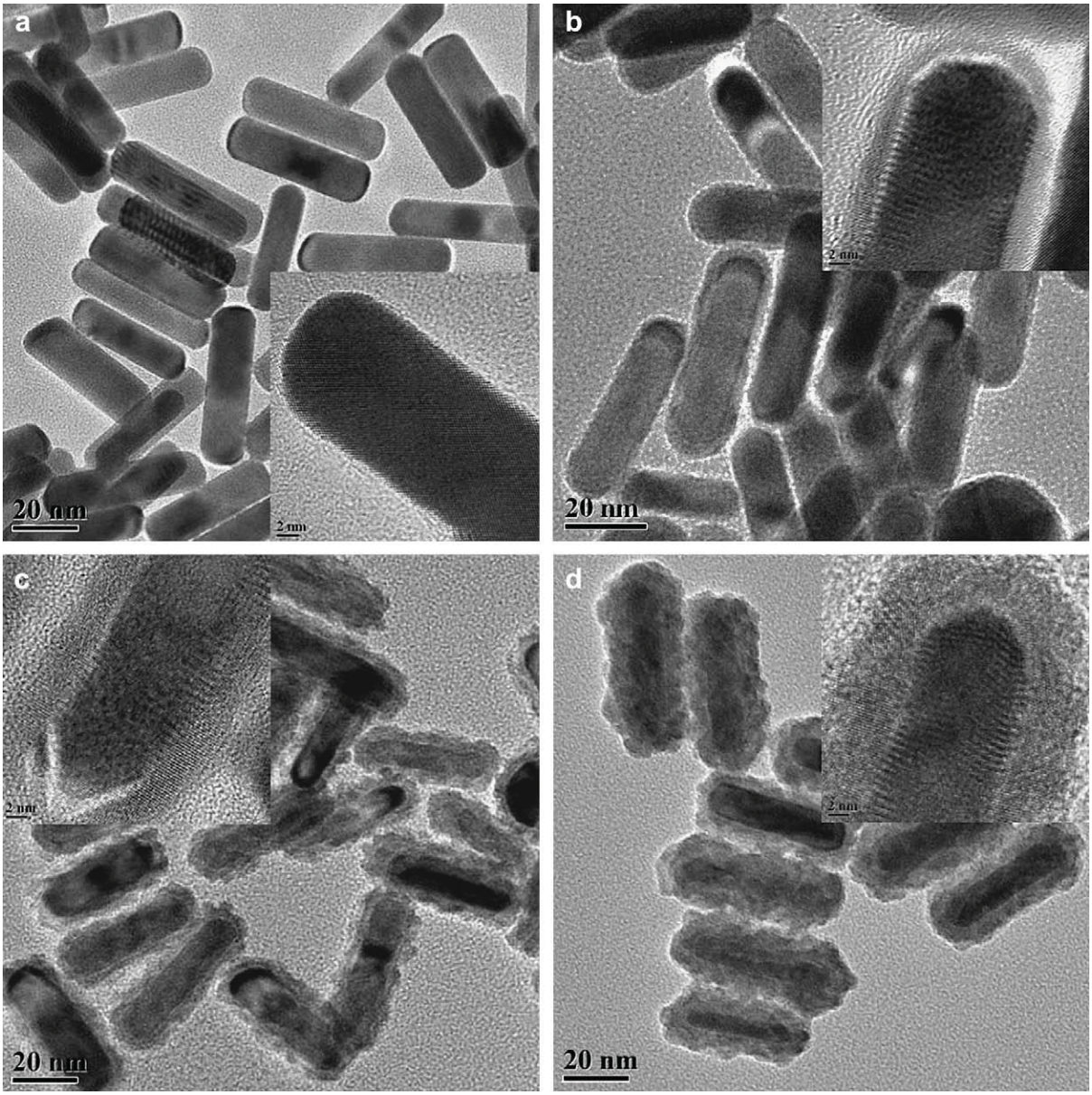

Fig. 2. TEM images obtained from the starting GNRs and the resulting gold nanorods coated with multiplex components: (a) Starting GNRs with LPW of 796 nm, (b,c,d) corresponding nanocomposite with LPW of 847, 989 and 1090 nm and the high resolution TEM images (inset figures).

few CTAB molecules on the ends in the CTAB solution, and the configuration facilitates selective modification of the GNRs [29,30]. During the formation of the Au_2S/AuAgS coated gold nanorods, there is no evidence of selective corrosion in the CTAB solution, and the shell is formed along the transverse and longitudinal directions at almost the same rate. Therefore, the nanorods do not evolve proportionally. Resonance light scattering (RLS) which can be used to monitor the changes of size and shape is used to characterize the nanocomposite and the results are depicted in Fig. 6. The GNRs display two RLS peaks centered at 450 and 570 nm attributable to the transverse and longitudinal surface plasmon resonance, respectively. The relative intensity of the scattering peaks from the nanorods with various LPWs discloses one important observation. The longer the LPW of the nanocomposite, the higher is the intensity of their first scattering band and the lower is the intensity of the second scattering band. Eventually, the second band disappears leaving only one observable band.

During the formation of the core–shell structure, the nanocomposite and thickness of the shell are controllable. Fig. 2 also shows the evolution of the starting GNRs and resulting nanocomposites. The starting GNRs exhibit a narrow size distribution as illustrated in Fig. 2a. In the first stage, the sulfide ions in the solution react with Au and Ag on the surface of the GNRs in the CTAB medium and the formed nano-shell covers the remaining GNR as shown in Fig. 2b. The thickness of the chalcogenide layer is controlled by the reaction time. The longer the reaction time, the thicker is the chalcogenide layer. Therefore, a further red shift in the LPW occurs until the excess Na_2S is removed from the solution. Fig. 2c and d illustrates that the Au_2S/AuAgS coated gold nanorods formed from the Au_2S/AuAgS coated gold nanorods shown in Fig. 2b further react with Na_2S. It indicates further formation of the chalcogenide layer inside the original shell along with reduction of the starting GNRs. It should be noted that this is different from that accomplished by conventional methods in which the formed layer

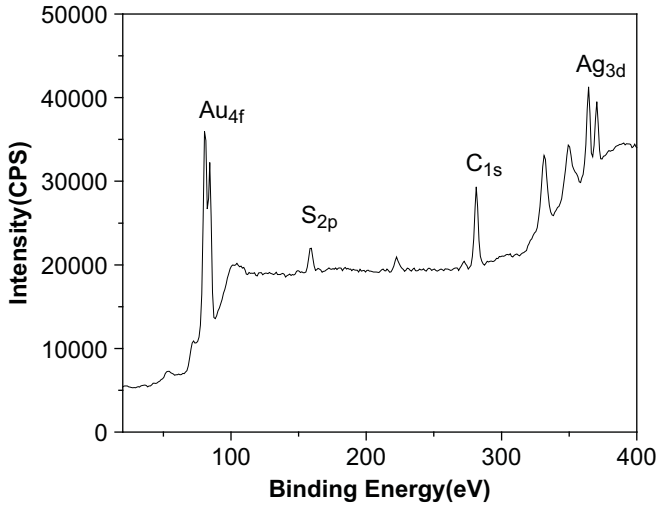

Fig. 3. XPS spectrum acquired from the gold nanorods coated with the multiplex components.

covers the shell. This means that the structure of the formed chalcogenide shell is looser allowing sulfide ions to penetrate through this layer. Thus, the reagent reacts with Au and Ag successively on the surface of the GNRs inside the layer and chalcogenide is generated subsequently. Formation of the chalcogenide layer by Na_2S occurs via reactions (1) and (2) in the CTAB medium as shown below. It is important for the solution to be in contact with air [31], as exemplified by the following reactions:

$$4Au + 2S^{2-} + O_2 + 2H_2O = 2Au_2S + 4OH^- \quad (1)$$

$$2Au + 2Ag + 2S^{2-} + O_2 + 2H_2O = 2AuAgS + 4OH^- \quad (2)$$

As aforementioned, the degree of red shift observed from the resulting nanorods depends on the reactant concentration, temperature, and reaction time. Although previous work reported that smaller concentration of Na_2S might stabilize GNRs in room temperature [32], in our experiments, under certain reactant concentrations, the red shift in the LPW is observed to be significantly enhanced by raising the temperature in the first stage and

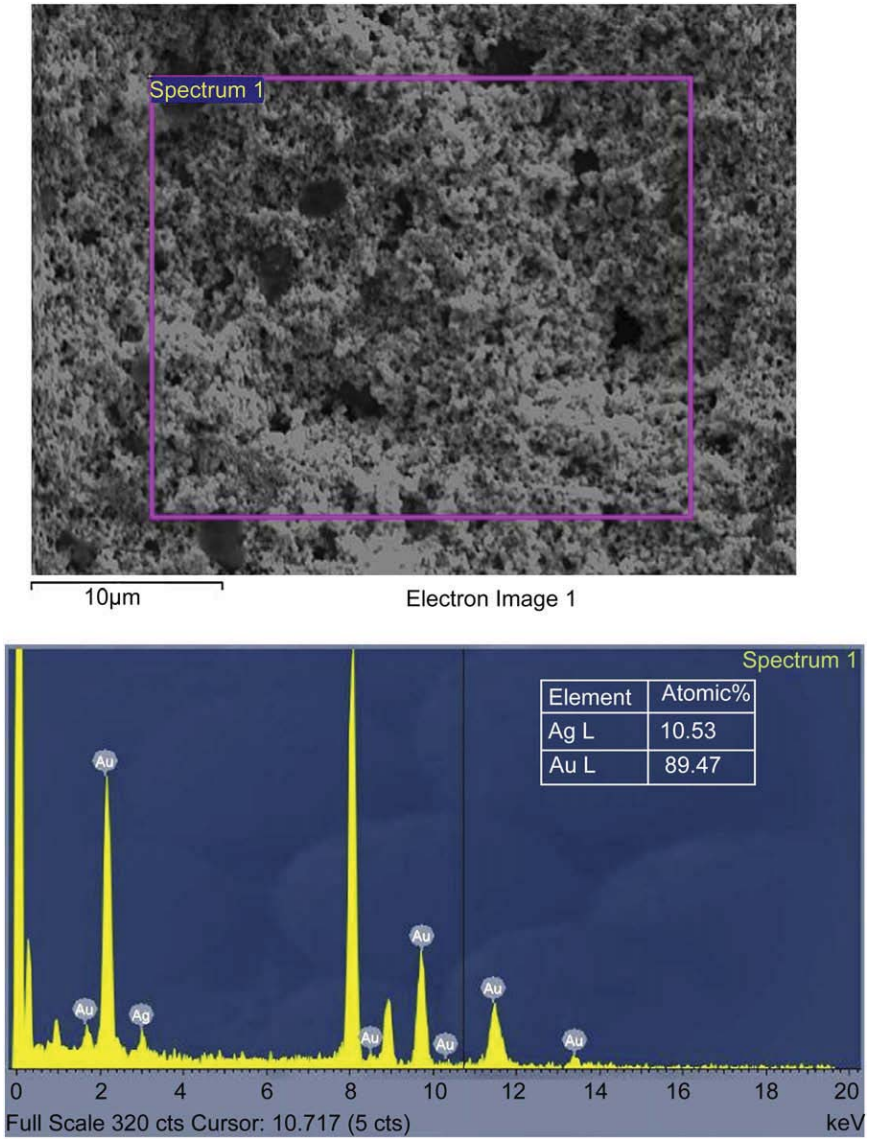

Fig. 4. Energy dispersive X-ray (EDS) spectrum of the as-synthesized GNRs.

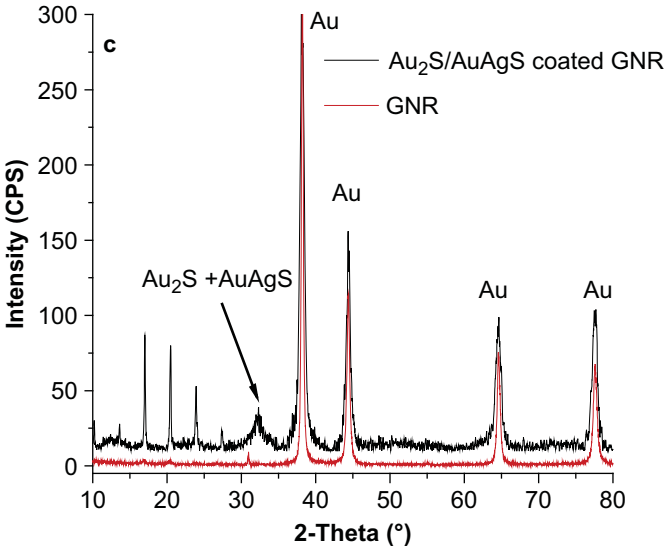

Fig. 5. Comparison of the XRD spectra between GNRs and Au_2S/AuAgS coated gold nanorods.

the rate of the red shift is linear with temperature. Upon further heating, the rate diminishes significantly and no distinct red shift can be observed even though the reaction proceeds for 5 min at 80 °C. However, a larger red shift will occur when this mixture is left for one day under room temperature because the sulfide ions can slowly penetrate the thicker chalcogenide layer to react with the remaining GNR inside the shell. In this work, a slightly excessive amount of ascorbic acid was added during the synthesis of gold nanorods. In order to eliminate possible interferences, pure gold nanorods resulting from resuspending the centrifuged as-synthesized gold nanorods into 0.1 M CTAB were subjected to similar experimental procedures. Our experimental results elucidate that there is no unwanted interference in the formation of Au_2S/AuAgS coated gold nanorods.

The final LPW of the formed nanocomposite depends on the aspect ratio of the remaining GNR and thickness of the shell. On the one hand, a red shift in the LPW occurs and the absorption intensity is attenuated as the chalcogenide layer is formed. This can be explained by the larger refractive indices of Au_2S and AuAgS thereby screening the incident electromagnetic field and changing the refractive index in the immediate vicinity of the GNRs. The EDS spectra of the Au_2S/AuAgS coated gold nanorods at various stages shown in Fig. 7 reveal that the amounts of the elemental S increase with thicker Au_2S/AuAgS layers, further demonstrating that the increasing shell results form the remaining GNRs reacting successively with sulfide ions penetrating through the formed chalcogenide layer. On the other hand, the generated chalcogenide shell in return reduces the GNR in all directions. The same corrosion rate in the transverse and longitudinal directions leads to an increase in the aspect ratio of the GNRs inducing the red shift from the starting nanorods. As illustrated in Fig. 2, an increase in the average aspect ratio of these remaining GNRs in the nanocomposites leading to red shifts in the LPW is observable at 3.8, 3.9, 5.1, and 5.5. Therefore, the degree of the red shift in the LPW of the Au_2S/AuAgS coated gold nanorods can be finely tuned over a larger range and indeed, our experiments show that LPW red shifts up to as much as 400 nm can be accomplished. In addition, the TPW red shift with increasing LPW is observed (Fig. 1), although the degree of the red shift in the TPW is less than that in the LPW. This method therefore renders a way by which the TPW can also be fine tuned thus boding well for potential optoelectronic and sensing applications.

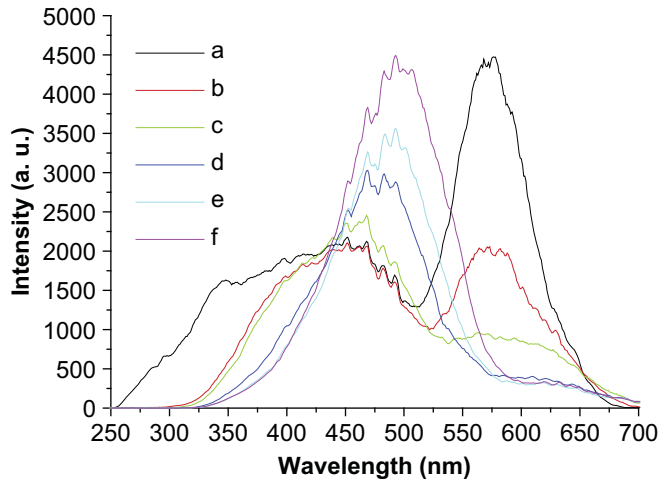

Fig. 6. Resonance light scattering spectra of GNRs reacting with Na_2S gradually, (a) represents GNR with LPW of 714 nm and (b, c, d, e) represent Au_2S/AuAgS coated gold nanorods with LPW of 741, 791, 893, 933, 963 nm, respectively.

As discussed above, Au_2S/AuAgS coated gold nanorods are produced from the as-synthesized with the addition of Na_2S in the CTAB solution, and red shifts are observed in the LPW. However, no red shift in the LPW can be observed if CTAB is removed. This simple reaction described here is exciting because of the following reasons. Firstly, this method introduces a novel concept to fabricate complex core–shell nanostructures. Secondly, this method provides high yield because the formation of core–shell structures from the starting gold nanoparticles proceed completely without any precipitation and aggregation among the nanoparticles. Thirdly, the process is very simple compared to conventional methods such as creation of a core with subsequent growth of a shell. It is particularly advantageous if the shell consists of multiplex components because other methods can be difficult and time consuming. Last but not least, both the thickness of the shell and size of the core can be readily controlled.

3.2. Optic properties of Au_2S/AuAgS coated gold nanorods

The properties associated with localized surface plasmon resonance from the nanocomposite are evaluated from the perspective of biological sensing. Firstly, the effects of different solvents on the GNRs and Au_2S/AuAgS coated gold nanorods are investigated. Three types of GNRs are studied: (1) LPW of 872 nm, (2) LPW of 850 nm and (3) LPW of Au_2S/AuAgS coated gold nanorods of 860 nm. Ethanol is added to the three types of nanorod suspensions to a volume ratio of water to ethanol of 1:1. A red shift in the LPWs of the nanorods is observed, namely 45 nm plasmon wavelength shift observed from the Au_2S/AuAgS coated gold nanorods. Similarly, 21 nm and 35 nm plasmon wavelength shifts corresponding to gold nanorods with LPWs of 872 nm and 850 nm are observed. The changes in the LPW indicate that the Au_2S/AuAgS coated gold nanorods are more sensitive to the changes in the environment and surrounding medium. Fig. 8 depicts the extinction spectra of the three types of nanorods dispersed in water and water/ethanol, respectively.

The Au_2S/AuAgS coated gold nanorods are investigated from the perspective of biosensors. Fig. 9 depicts the extinction spectra after the gradual addition of glucose to the GNRs and Au_2S/AuAgS coated gold nanorods. The two types of nanorods exhibit similar behavior.

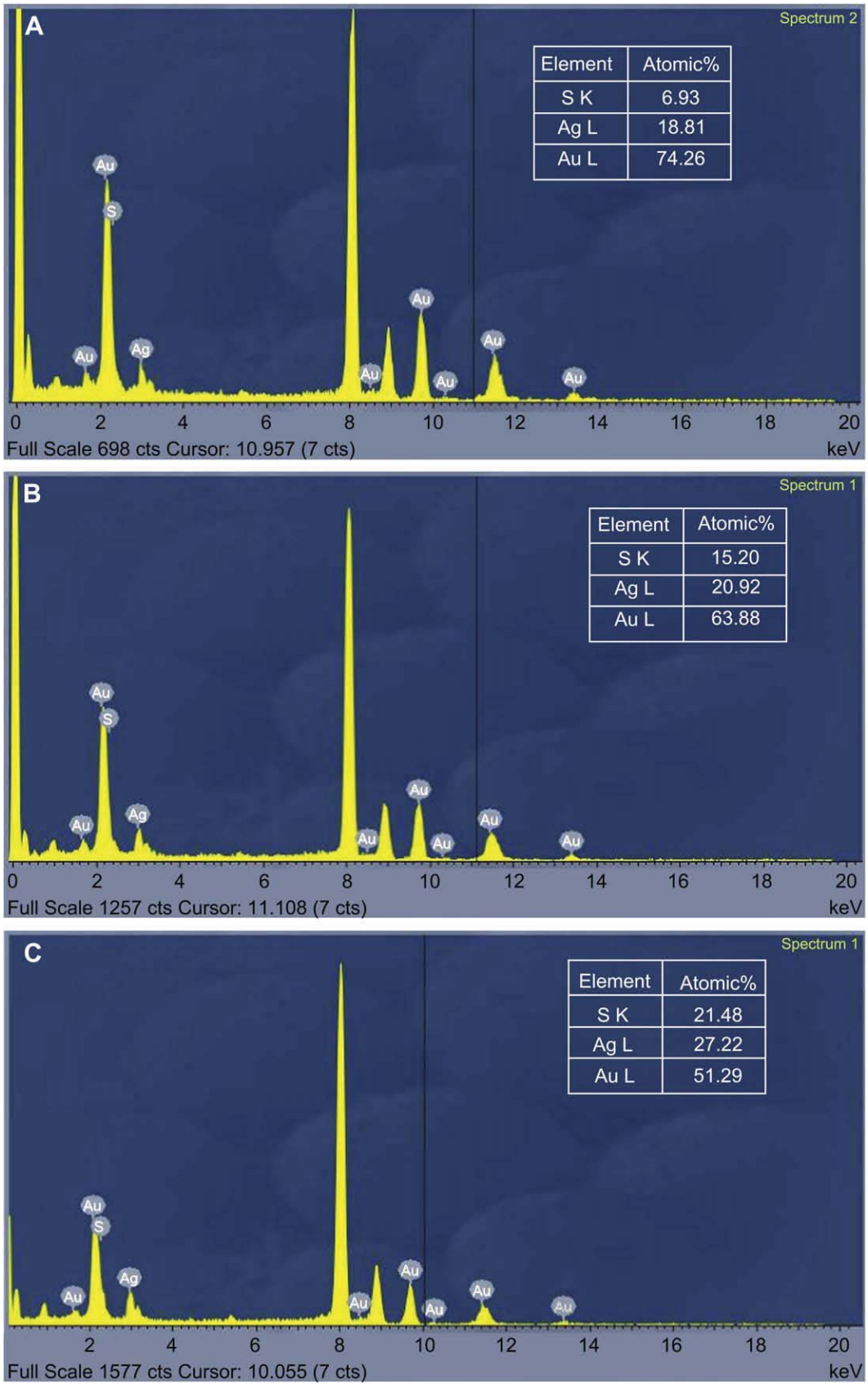

Fig. 7. EDS spectra of gold nanorods coated with different thicknesses of Au_2S/AuAgS showing (A) LPW 847, (B) 989, and (C) 1090 nm corresponding to Fig. 2.

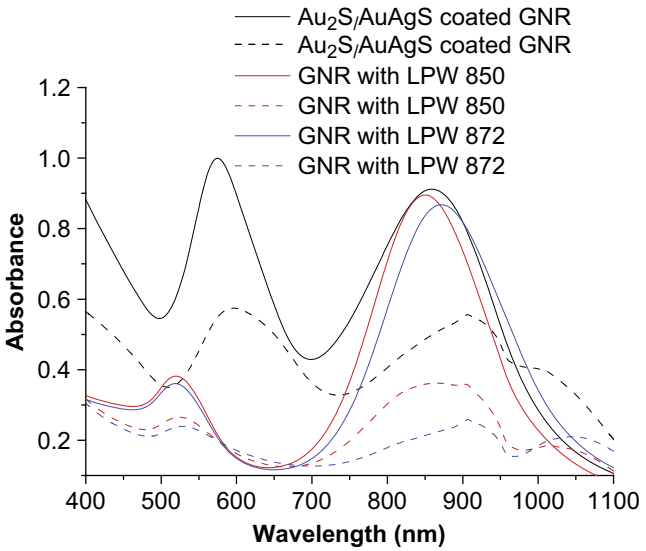

Fig. 8. Extinction spectra of the three types of nanorods dispersed in water and water/ethanol (1:1) with solid lines representing in water and dash lines in water/ethanol (1:1).

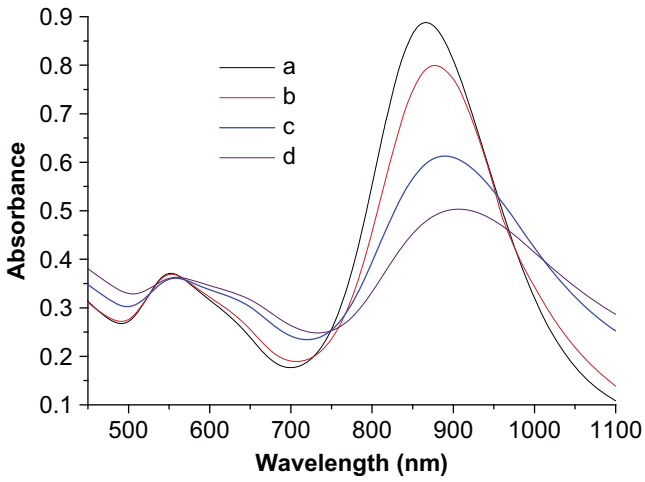

Fig. 10. Extinction spectra acquired by rabbit anti-goat IgG binding to the goat IgG attached on the Au_2S/AuAgS coated gold nanorods: (a) Au_2S/AuAgS coated gold nanorods, (b) Au_2S/AuAgS coated gold nanorods modified by MUA, (c) goat IgG attached on the Au_2S/AuAgS coated gold nanorods-MUA, (d) 3 nM of rabbit anti-goat IgG in the solution binding to goat IgG on the Au_2S/AuAgS coated gold nanorod optical biosensor.

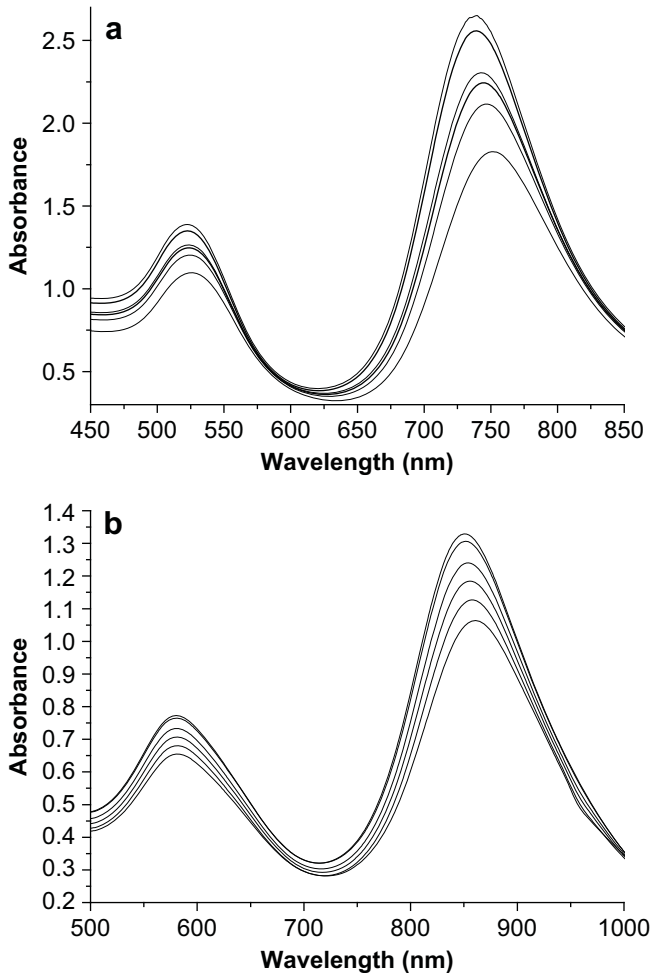

Fig. 9. Effects of concentrations of glucose on GNRs (a) and Au_2S/AuAgS coated gold nanorods (b). The concentration of glucose increases gradually from top to bottom and the concentration of nanorods decrease gradually with addition of the glucose solution.

The LPW red shifts but the absorption intensity decreases due to the reduced nanorod concentration as a result of addition of glucose.

3.3. Functionalization of Au_2S/AuAgS coated gold nanorods and detection of biological targets

Functionalization of the Au_2S/AuAgS coated gold nanorods takes advantage of the affinity between the Au_2S/AuAgS and thiol compounds. It should be noted that the formation of alkanethiol SAM introduces a red shift in the plasmon peaks on account of changes in the refractive index in the vicinity of the Au_2S/AuAgS coated gold nanorods. Fig. 10 displays the spectra of the nanorod suspension before and after alkanethiol (mercaptoundecanoic acid, MUA) attachment. A red shift of 7 nm in the longitudinal peak is clearly identified indicating formation of alkanethiol SAM. Repeated measurements performed on the same nanorod sample over 2 days yields a maximum peak drift of 0.5 nm, indicating that the 7 nm red shift can only be caused by SAM formation.

After the SAM of MUA is formed, biomolecules can be covalently attached via the NH_2 bond of the antibodies to the NHS-terminated nanorods. A further red shift of the plasmon peak can be observed. The same nanorods after the goat IgG attachment show a significant shift (of up to 20 nm) compared to the unmodified nanorods. The sensitivity of the plasmon spectra of the nanorods to the attachment of layers of molecules forms the basis of molecular biosensors using single particles. Fig. 10 also depicts the detection of rabbit anti-goat IgG using the Au_2S/AuAgS coated gold nanorods attached by goat IgG via plasmon shifts. The transverse plasmon peaks near 575 nm are not very sensitive to the refractive index change induced by target binding, and the red shift of these peaks is below 3 nm. Hence, it is difficult to detect specific target binding. Akin to common GNRs [33,34], the longitudinal peaks of the Au_2S/AuAgS coated gold nanorods are extremely sensitive to the refractive index changes induced by target binding. Therefore, they are excellent sensors for target-specific binding events and have the potential to achieve single-molecule sensitivity in micro-spectroscopy. When a sample is added, the Au_2S/AuAgS coated gold nanorods tagged with the probe interact specifically with this target resulting in a significant red shift of up to 20 nm in the longitudinal plasmon peak.

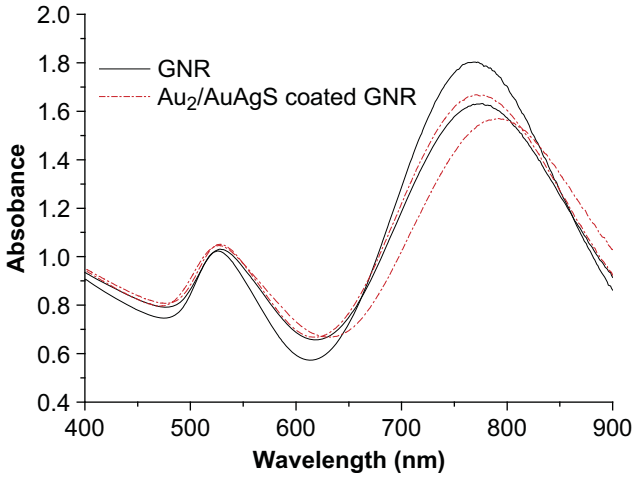

Fig. 11. Extinction spectra acquired before and after BSA attachment onto the gold nanorods and Au_2S/AuAgS coated gold nanorods.

Control experiments were carried out in order to further prove the high sensitivity of Au_2S/AuAgS coated gold nanorods. Two types of nanorods, gold nanorods with LPW 769 nm and Au_2S/AuAgS coated gold nanorods with LPW 770 nm were selected to investigate, respectively. Significant red shift of plasmon peaks of the absorption curves corresponding to the two types of nanorods attached with biological molecule can be observed, as shown in Fig. 11. From this figure, it can be seen that the Au_2S/AuAgS coated gold nanorods display 18 nm wavelength shifts while gold nanorods 12 nm after the attachment of BSA. Apparently, Au_2S/AuAgS coated gold nanorods show larger plasmon wavelength shift than the gold nanorods under the same experimental conditions. Therefore, comparing to the common gold nanorods, these results show the Au_2S/AuAgS coated gold nanorods exhibit higher sensitivity.

4. Conclusion

Au_2S/AuAgS coated gold nanorods are produced with the addition of Na_2S in the CTAB solution, and red shifts are observed in the LPW. However, no red shift in the LPW can be observed if CTAB is removed. This simple technique can be used to conveniently fabricate complex core–shell nanostructures with a high yield because the formation of core–shell structures with controllable shell thickness and core size proceed completely without any precipitation and aggregation among the nanoparticles. Hence, the plasmon resonance of the nanocomposite can be tuned over a range of several hundred nanometers. These Au_2S/AuAgS coated gold nanorods are more sensitive to changes of the environment and medium compared to other common GNRs. Our experimental results demonstrate that Au_2S/AuAgS coated gold nanorods have excellent properties in sensing specific target binding events since significant changes occur in the plasmon spectra in response to a change in the refractive index in the vicinity of nanocomposite. The materials are thus useful in many emerging applications including biolabels, chemical sensing, surface enhanced Raman scattering, and so on.

Acknowledgements

This work was jointly supported by Scientific Research Fund of Hunan Provincial Education Department (06B028), National Basic Research Fund (2005CB623901), National Natural Science Foundation of China (30700170, 20772027, 20803020), Shanghai Science and Technology R&D Fund (07QH14016, 07JC14057), Innovation Fund of SICCAS (SCX0606), and Hong Kong Research Grants Council (RGC) General Research Funds (GRF) No. CityU 112307.

Appendix

Figures with essential colour discrimination. Most of the figures in this article have parts that are difficult to interpret in black and white. The full colour images can be found in the on-line version, at doi:10.1016/j.biomaterials.2009.06.060.

References

[1] Cozzoli PD, Curri ML, Giannini C, Agostiano A. Synthesis of TiO_2–Au composites by titania-nanorod-assisted generation of gold nanoparticles at aqueous/nonpolar interfaces. Small 2006;2:413–21.
[2] Bartl MH, Boettcher SW, Frindell KL, Stucky GD. 3-D molecular assembly of function in titania-based composite material systems. Acc Chem Res 2005;38:263–71.
[3] Nandanan E, Jana NR, Ying JY. Functionalization of gold nanospheres and nanorods by chitosan oligosaccharide derivatives. Adv Mater 2008;20:2068–73.
[4] Jana NR. Gram-scale synthesis of soluble, near-monodisperse gold nanorods and other anisotropic nanoparticles. Small 2005;1:875–82.
[5] El-Sayed MA. Small is different: shape-, size-, and composition-dependent properties of some colloidal semiconductor nanocrystals. Acc Chem Res 2004;37:326–33.
[6] Dong Y, Yu G, McAlpine MC, Lu W, Lieber CM. Si/a-si core/shell nanowires as nonvolatile crossbar switches. Nano Lett 2008;8:386–91.
[7] Huang YF, Chang HT, Tan W. Cancer cell targeting using multiple sptamers conjugated on nanorods. Anal Chem 2008;80:567–72.
[8] Nie Z, Fava D, Rubinstein M, Kumacheva E. 'Supramolecular' assembly of gold nanorods end-terminated with polymer 'pom-poms': effect of 'pom–pom' structure on the association modes. Am Chem Soc 2008;130:3683–9.
[9] Bakalova R, Ohba H, Zhelev Z, Ishikawa M, Baba Y. Quantum dots as photosensitizers. Nat Biotechnol 2004;22:1360–1.
[10] Patolsky F, Zheng G, Lieber CM. Nanowire sensor for medicine and the life science. Nanomedicine 2006;1:51–65.
[11] Hauck TS, Jennings TL, Yatsenko T, Kumaradas JC, Chan WCW. Enhancing the toxicity of cancer chemotherapeutics with gold nanorod hyperthermia. Adv Mater 2008;20:2832–8.
[12] Gao JX, Bender CM, Murphy CJ. Dependence of the gold nanorod aspect ratio on the nature of the directing surfactant in aqueous solution. Langmuir 2003;19:9065–70.
[13] Nikoobakht B, El-Sayed MA. Preparation and growth mechanism of gold nanorods (NRs) using seed-mediated growth method. Chem Mater 2003;15:1957–62.
[14] Sastry M, Rao M, Ganesh KM. Electrostatic. assembly of nanoparticles and biomacromolecules. Acc Chem Res 2002;35:847–55.
[15] Kolny J, Kornowski A, Weller H. Self-organization of cadmium sulfide and gold nanoparticles by electrostatic interaction. Nano Lett 2002;2:361–4.
[16] Yi DK, Selvan ST, Lee SS, Papaefthymiou GC, Kundaliya D, Ying JY. Silica-coated nanocomposites of magnetic nanoparticles and quantum dots. J Am Chem Soc 2005;127:4990–1.
[17] Milliron DJ, Hughes M, Cui Y, Manna L, Li J, Wang LW, et al. Colloidal nanocrystal heterostructures with linear and branched topology. Nature 2004;430:190–5.
[18] Molari T, Rothenberg E, Popov I, Costi R, Banin U. Selective growth of metal tips onto semiconductor quantum rods and tetrapods. Science 2004;304:1787–90.
[19] Yu H, Chen M, Rice PM, Wang SX, White RL, Sun S. Dumbbell-like bifunctional Au–Fe_3O_4 nanoparticles. Nano Lett 2005;5:379–82.
[20] Wang C, Ma Z, Wang T, Su Z. Synthesis, assembly, and biofunctionalization of silica-coated gold nanorods for colorimetric biosensing. Adv Funct Mater 2006;16:1673–8.
[21] Brioude A, Jiang XC, Pileni MP. Optical properties of gold nanorods: DDA simulations supported by experiments. J Phys Chem B 2005;109:13138–42.
[22] Gou L, Murphy CJ. Fine-tuning the shape of gold nanorods. Chem Mater 2005;17:3668–72.
[23] Ishikawa K, Isonaga T, Wakita S, Suzuki Y. Structure and electrical properties of Au_2S. Solid State Ionics 1995;79:60–6.
[24] Gurevich VM, Gavrichev KS, Gorbunov VE, Baranova NN, Tagirov BR, Golushina LN, et al. The heat capacity of Au_2S(cr) at low temperatures and derived thermodynamic functions. Thermochim Acta 2004;412:85–90.
[25] Zotov AV, Baranova NN, Bannykh LN. Solubility of the gold sulfides Au_2S and AgAuS in solutions containing hydrogen sulfide at 25–80 °C and pressures of 1 and 500 bar. Geochem Int 1996;34:216–21.
[26] Osadchii EG, Rappo OA. Determination of standard thermodynamic properties of sulfides in the Ag–Au–S system by means of a solid-state galvanic cell. Am Miner 2004;89:1405–10.
[27] Averitt RD, Sarkar D, Halas NJ. Plasmon resonance shifts of Au-coated Au_2S nanoshells: insight into multicomponent nanoparticle growth. Phys Rev Lett 1997;78:4217–20.

[28] Zhai HJ, Bürgel C, Bonacic-Koutecky V, Wang LS. Probing the electronic structure and chemical bonding of gold oxides and sulfides in AuOn(−) and AuSn(−) ($n = 1, 2$). J Am Chem Soc 2008;130:9156–67.
[29] Daniel MC, Astruc D. Gold nanoparticles: assembly, supramolecular chemistry, quantum-size-related properties, and applications toward biology, catalysis, and nanotechnology. Chem Rev 2004;104:293–346.
[30] Térez-Juste J, Pastoriza-Santos I, Liz-Marzán LM, Vaney P. Gold nanorods: synthesis, characterization and applications. Coordin Chem Rev 2005;249:1870–901.
[31] Liu M, Guyot-Sionnest P. Preparation and optical properties of silver chalcogenide coated gold nanorods. J Mater Chem 2006;16:3942–5.
[32] Zweifel DA, Wei A. Sulfide-arrested growth of gold nanorods. Chem Mater 2005;17:4256–61.
[33] Yu C, Irudayaraj J. Multiplex biosensor using gold nanorods. Anal Chem 2007;79:572–9.
[34] Marinakos SM, Chen S, Chilkoti A. Plasmonic detection of a model analyte in serum by a gold nanorod sensor. Anal Chem 2007;79:5278–83.